Probing particle-phonon-coupled states in the neutron-rich nucleus ^{65}Cu by lifetime measurements with fast-timing techniques

G. Bocchi,[1] S. Leoni,[1,2] S. Bottoni,[1,2] G. Benzoni,[2] A. Bracco,[1,2] P. F. Bortignon,[1,2] G. Colò,[1,2] B. Belvito,[1] C. R. Niţă,[3] N. Marginean,[3] D. Filipescu,[3] D. Ghita,[3] T. Glodariu,[3] R. Lica,[3] R. Marginean,[3] C. Mihai,[3] A. Negret,[3] T. Sava,[3] L. Stroe,[3] S. Toma,[3] D. Bucurescu,[3] I. Georghe,[3] R. Suvăilă,[3] D. Deleanu,[3] C. A. Ur,[4] and S. Aydin[5]

[1]*Dipartimento di Fisica, University of Milano, Milano, Italy*

[2]*INFN, Sezione di Milano, Milano, Italy*

[3]*Horia Hulubei National Institute of Physics and Nuclear Engineering - IFIN HH, Bucharest, 077125, Romania*

[4]*INFN Sezione di Padova, Padova, Italy*

[5]*Department of Physics, University of Aksaray, Aksaray, Turkey*

(Received 4 March 2014; published 2 May 2014)

The ^{65}Cu nucleus was populated by the ^{64}Ni(^{7}Li,α2n)^{65}Cu reaction and the lifetime of the $9/2^+$ state at 2.5 MeV was measured by electronic fast-timing technique, providing the value $\tau = 37(3)$ ps. The reduced transition probability $B(E3) = 8.82(165)$ W.u. is deduced and compared to theoretical predictions in the framework of a particle-vibration (weak) coupling model. The results indicate that the $9/2^+$ state is a member of the $3^- \otimes \pi p3/2$ multiplet, built by coupling the octupole 3^- phonon of ^{64}Ni to an unpaired proton in the $p_{3/2}$ level, confirming the robustness of core excitations in the medium mass nucleus ^{64}Ni.

DOI: 10.1103/PhysRevC.89.054302 PACS number(s): 25.70.Hi, 23.20.Lv, 21.10.Tg, 27.50.+e

I. INTRODUCTION

Neutron-rich Cu nuclei, with one proton outside the closed shell at $Z = 28$, provide valuable information on nuclear structure around the Ni shell closure [1–4]. In particular, single- and few-particle excitations reveal the rigidity of the closed shell core and can be used to test, in great detail, modern shell-model calculations. In addition, states arising by coupling the unpaired proton to phonon excitation of the core can also be probed: these are key ingredients to explain important phenomena, such as the observed reduction of spectroscopic factors, the anharmonicity of vibrational spectra, the damping of giant resonances, etc. [5,6]. Examples of particle-phonon coupled states have recently been found in the Ca region, around $N = 28$, where, in particular, low-lying positive parity states in ^{49}Ca and ^{47}Ca have been successfully interpreted within this framework [7,8]. This has shown the possibility of robust core excitations in medium mass nuclei, although additional experimental observation should be obtained in order to draw more general conclusions.

In this work, we present the results of the measurement, by electronic fast-timing technique [9], of the $9/2^+$ state in ^{65}Cu, which is candidate to be a member of the $3^- \otimes \pi p3/2$ multiplet, built by coupling the octupole 3^- phonon of ^{64}Ni to the unpaired proton in the $p_{3/2}$ level. In addition, the lifetimes of few excited states in ^{68}Ga, populated in the same reaction, have also been measured. The experimental setup and the details of the lifetime measurements are discussed in Secs. II and III, while in Sec. IV a theoretical interpretation of the $9/2^+$ state, within a particle-vibration coupling (PVC) model, is presented.

II. EXPERIMENT

The ^{65}Cu nucleus was populated in the ^{64}Ni(^{7}Li,α2n)^{65}Cu reaction induced by a ^{7}Li beam onto a thick, highly enriched, and self-supported ^{64}Ni target, at an incident energy of 32 MeV. The ^{7}Li beam was delivered by the Tandem accelerator (9 MV) of the Horia Hulubei National Institute of Physics and Nuclear Engineering (IFIN-HH) in Bucharest and the γ rays were detected using the mixed ROSPHERE setup, which consisted of 14 HPGe detectors of 50% relative efficiency and 11 $LaBr_3$(Ce) detectors (of different crystal dimensions, 2 in. $\times$ 2 in., 1.5 in. $\times$ 1.5 in., and 1 in. $\times$ 1.5 in. $\times$ 1.5 in. of conical shape), all placed in five rings at $\theta = 37^\circ$, 70°, 90°, 110°, and 143° with respect to the beam axis. This corresponds to an absolute detection efficiency at 1.33 MeV of $\approx$1.5% and $\approx$1%, for HPGe and $LaBr_3$(Ce) detectors, respectively.

The time spectrum of the $LaBr_3$(Ce) detectors was carefully corrected for the time-walk effect, following the procedure presented in details in Refs. [9,10] and briefly illustrated in Fig. 1. In the left column of the figure, a two-dimensional energy vs time matrix is shown, as measured by one $LaBr_3$(Ce) detector of the ROSPHERE array, using a ^{60}Co source and requiring a coincidence with the 1332 keV full energy peak in one $LaBr_3$(Ce) (chosen as a reference). The entire energy range, including the full energy coincidence peak (at 1173 keV) and the associated (continuum) Compton scattered events corresponds to prompt γ rays. Such energy range has been divided into small energy intervals ($\approx$200 keV wide) and the position of the corresponding time peak has been interpolated linearly. This provides a correction to the time centroid as a function of E_γ. As shown in the right column of Fig. 1, for three selected energy regions, the energy dependence in the time spectra is eliminated, resulting in an average time resolution of the $LaBr_3$(Ce) detectors of $\approx$300 ps.

From the analysis of the lowest spin transitions collecting the majority of the decay flux of the populated nuclei, it is found that the most intense channels are those leading to the formation of ^{65}Cu ($\alpha 2n$), ^{69}Ga ($2n$), ^{68}Ga ($3n$), and ^{67}Zn ($p3n$), with relative intensities of the order of 52%, 32%, 13%, and <5%, respectively. Figure 2 shows a spectrum of ^{65}Cu

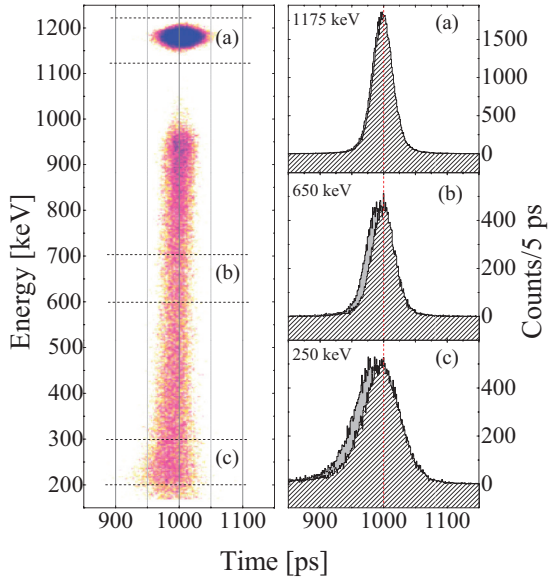

FIG. 1. (Color online) Left side: Energy vs time (5 ps/ch) matrix measured by one $LaBr_3$(Ce) detector of the ROSPHERE array, using a ^{60}Co source and requiring a coincidence with the 1332 keV full energy peak in a given $LaBr_3$(Ce) crystal (chosen as a reference). The matrix has been obtained after applying a time-walk correction to the entire energy window, along the Compton edge, up to the photo peak at 1173 keV. Right side: projections of the time spectrum relative to three representative energy regions, 100 keV wide, around the photo peak (a), at 650 (b) and at 250 keV (c). The dark (light) histogram represents the time distribution before (after) the time walk correction (see text for details).

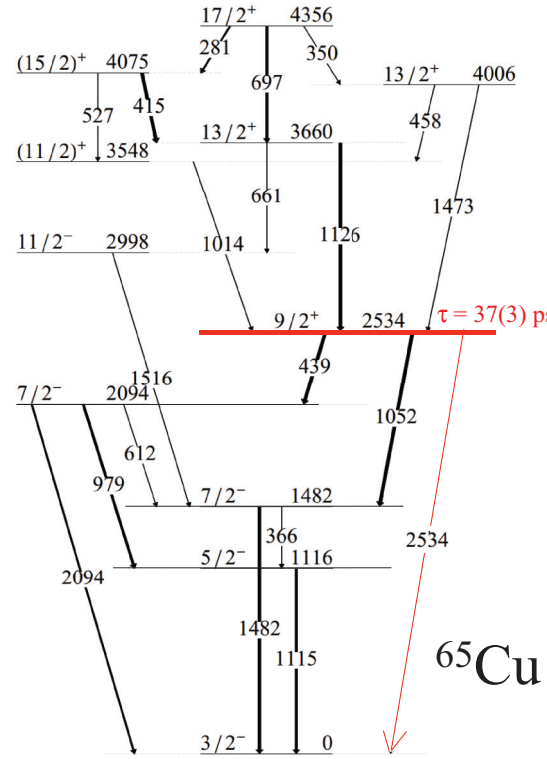

FIG. 3. (Color online) Partial level scheme of ^{65}Cu, as follows from the work of Ref. [11], showing the relevant levels populated in the present reaction. The $9/2^+$ level of interest for the present lifetime measurement is indicated by thick (red) line.

obtained from the HPGe detectors, requiring a coincidence with the 415 keV line, depopulating the $(15/2^+)$ level of ^{65}Cu at 4075 keV. As indicated by labels, all strong transitions belong to ^{65}Cu, apart from few contaminant lines of ^{68}Ga. The partial level scheme of ^{65}Cu, relevant for this work, is shown in Fig. 3 [11].

In the following section, the lifetime analysis of the $9/2^+$ state of ^{65}Cu and of a few excited states of ^{68}Ga is presented.

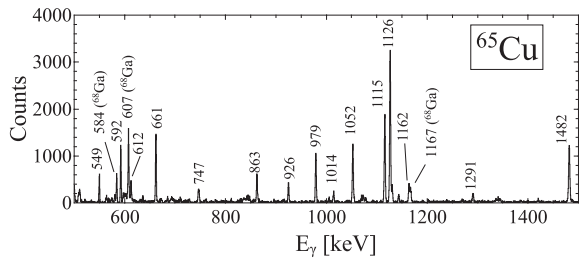

FIG. 2. Energy spectrum of ^{65}Cu measured with the HPGe detectors, with a coincidence requirement on the 415 keV transition of ^{65}Cu. Labels mark the strongest transitions of ^{65}Cu and contaminant lines of ^{68}Ga (cf. the level schemes given in Figs. 3 and 6).

III. EXPERIMENTAL RESULTS

The mixed ROSPHERE array, being made of HPGe and fast $LaBr_3$(Ce) scintillator detectors, enables efficient triple γ coincidence measurements, with one γ detected in the HPGe array (to cleanly select a given γ cascade) and two γ's in the $LaBr_3$(Ce) system. The latter are used to determine the lifetime of the excited state of interest, by constructing a Δt time spectrum between the γ rays which populate, and subsequently, deexcite a specific state. The data are sorted into $E_{\gamma,\text{stop}}$-$E_{\gamma,\text{start}}$-Δt cubes using the GASPWARE software package [12], where $E_{\gamma,\text{stop}}$ and $E_{\gamma,\text{start}}$ represent the energy measured in the $LaBr_3$(Ce) detectors. After a careful subtraction of the background associated to the energy gate (as shown in Fig. 4 for the present work) [9], the lifetime is obtained by fitting the Δt time distribution by a convolution of two functions: a Gaussian, representing the intrinsic time resolution of the detection system, and an exponential function describing the law of radioactive decay. The lifetime value can be typically extracted by interpolating the exponential slope but, for lifetime shorter or comparable with the time resolution, the prompt distribution is the main component of the convolution. In this case, the displacement of the centroid can be used to determine the lifetime value by measuring its shift with respect to the prompt peak [9].

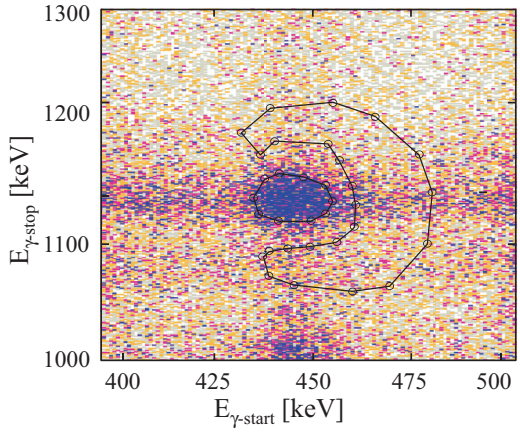

FIG. 4. (Color online) Example of a selected energy window of the symmetric ($LaBr_3$-$LaBr_3$) coincidence matrix, obtained as a projection of the $E_{\gamma,\text{stop}}$-$E_{\gamma,\text{start}}$-Δt cube constructed for the lifetime analysis of the $9/2^+$ state of ^{65}Cu. It shows the coincidence relationship between the pairs of γ rays of 1126 and 439 keV, populating and depopulating the $9/2^+$ states of interest, respectively (cf. Fig. 3). The solid contour lines indicate the peak and background gating regions.

A. Lifetime analysis of the $9/2^+$ state at 2534 keV in ^{65}Cu

In the case of ^{65}Cu, the lifetime of the $9/2^+$ state at 2534 keV has been measured. This state is a candidate for being a coupling between the unpaired $p_{3/2}$ proton of ^{65}Cu and the 3^- octupole phonon of the ^{64}Ni core. Following the procedure outlined above, all possible triple combinations of γ rays have been considered in order to determine the start and stop pairs in the $LaBr_3$(Ce) detectors and the HPGe energy gating condition. This resulted in the combinations listed in Table I, which allowed us to maximize the statistics collected in the final Δt time spectrum. For each triple-γ combination it has been checked that the HPGe gating condition was not introducing any bias in the Δt spectrum, namely that the lifetime of the level involved in the gating condition

TABLE I. Combinations of triple E_γ(HPGe)-$E_{\gamma,\text{start}}$($LaBr_3$)-$E_{\gamma,\text{stop}}$($LaBr_3$) coincidences used in the lifetime analysis of the $9/2^+$ state of ^{65}Cu (cf. Fig. 3).

E_γ(HPGe) (keV)	$E_{\gamma,\text{start}}$($LaBr_3$) (keV)	$E_{\gamma,\text{stop}}$ ($LaBr_3$) (keV)
415	281	1115
	281	1482
439	281	1115
	281	1482
	415	1115
979	281	1115
	415	439
1126	415	439
	415	1052
	415	1115

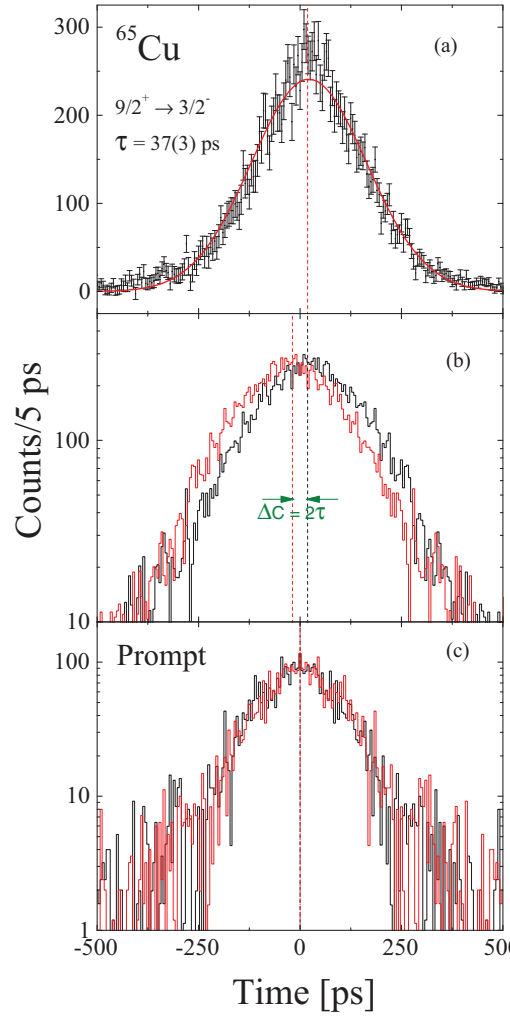

FIG. 5. (Color online) (a) Time distribution of the $9/2^+$ state of ^{65}Cu. The thick (red) line is the fit of the experimental data by the convolution function discussed in the text. (b) Time distribution obtained by considering the difference $t_{\text{stop}} - t_{\text{start}}$ (thin (black) line) and corresponding $t_{\text{start}} - t_{\text{stop}}$ time spectrum [thick (red) line]. The displacement ΔC of the two centroids is also indicated, from which the direct measurement of the lifetime of the state can be obtained. (c) Time distributions obtained by considering start-stop combinations of prompt γ rays, where no displacement is seen.

was within the energy resolution of the $LaBr_3$(Ce) system ($\sim$300 ps).

The top panel of Fig. 5 shows the time spectrum obtained for the $9/2^+$ state of ^{65}Cu, summing over all triple γ-combinations listed in Table I. Since the time distribution does not show a pronounced tail, the lifetime of the state has been evaluated directly from the shift of the centroid, as illustrated in the bottom panel of the same figure. A lifetime of $\tau = 37(3)$ ps is found, which corresponds to $B(E3) = 8.82(165)$ W.u., after taking into account the $\approx$3% decay branching of the $9/2^+$ state to the $3/2^-$ ground state, given in Ref. [11]. This value is rather close, within the error, to the $B(E3)$ value of the 3^- octupole phonon of the ^{64}Ni core, reported to be 10.83(59) W.u. [13]. It is interesting to note that

in the case of ^{67}Cu, the half-life of the $9/2^+$ state has been recently measured by fast-timing techniques with the ROSPHERE array [10], providing the experimental half-life value $T_{1/2} = 157(15)$ ps. This corresponds to $B(E3) = 16.8(17)$ W.u., after taking into account the ≈35 % decay branch of the $9/2^+$ state to the $3/2^-$ ground state, established in Ref. [11]. In this case, no experimental measurement of the $B(E3)$ strength of the 3^- octupole phonon of the ^{66}Ni core is available. Therefore, it becomes very interesting to perform theoretical calculations for the cases of ^{65,67}Cu, within, e.g., the framework of the particle-phonon coupling model [5], as discussed in Sec. IV.

B. Lifetime analysis of excited states in ^{68}Ga

Among the strongest populated nuclei in the present experiment, ^{68}Ga was the least known in terms of lifetime

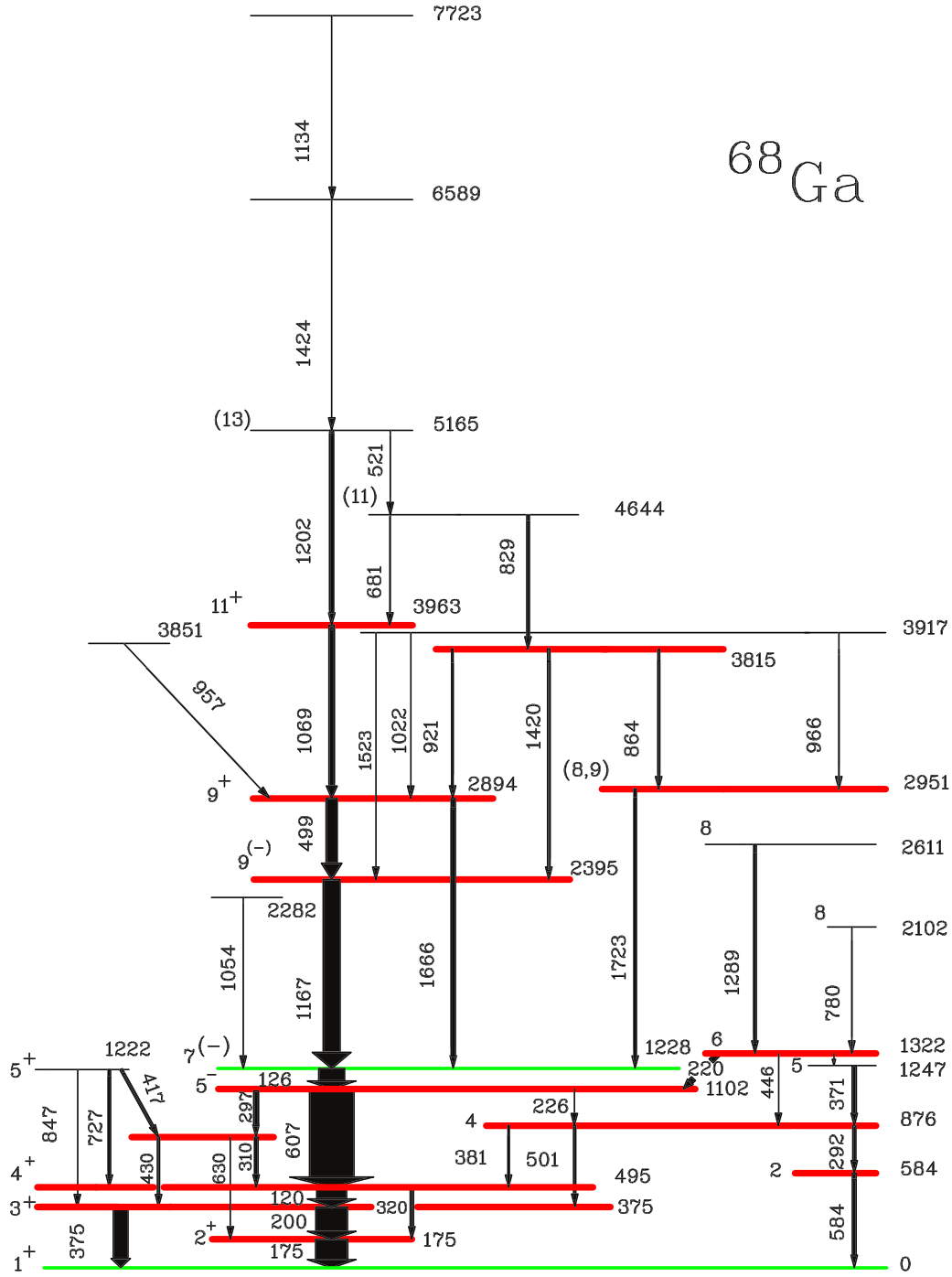

FIG. 6. (Color online) Level scheme of ^{68}Ga, according to the work of Ref. [15]. The lifetime values of the levels, marked by thick (red) lines, have been determined in the present work and they are reported in Table II. From previous works only the lifetimes of the 1^+ and $7^{(-)}$ states (in green) were known [14] (adapted from Ref. [15]).

TABLE II. Lifetimes values of excited states of ^{68}Ga, obtained in this work by fast timing techniques. Energy, spin and parity of each state, given in the first and second column, are taken from Ref. [14].

E_{level} (keV)	J_i^π	τ
175.0	2^+	3.37 ± 0.11 ns
375.6	3^+	2.87 ± 0.04 ns
496.1	4^+	<30 ps
583.8	2^-	<30 ps
806.2	4^+	<30 ps
876.8	4^-	527.42 ± 22.63 ps
1103.5	5^-	214.46 ± 2.80 ps
1323.2	6^-	187.21 ± 17.21 ps
2396.8	$9^{(-)}$	298.90 ± 5.76 ps
2896.1	9^+	226.00 ± 8.27 ps
2953.2	$(8,9^-)$	<30 ps
3817.6	(9)	103.15 ± 17.40 ps
3965.0	11^+	<30 ps

of the excited states. As shown in Fig. 6, prior to this work only the ground state and the $7^{(-)}$ isomeric state at 1228 keV had a measured half-life (of 67.7 m and 62 ns, respectively), while for few other levels an upper limit of 5 ns was given [14]. Making use of the fast-timing techniques based on the triple-γ coincidences with HPGe and $LaBr_3$(Ce) detectors, described at the beginning of this section, the lifetime of eight excited states has been determined, while for other five levels the upper limit of 30 ps was deduced, as shown in Table II.

Figure 7 shows, as an example, the time distributions obtained for the 375 keV, 876 keV, and 175 keV states of ^{68}Ga.

The structure of the odd-odd ^{68}Ga nucleus has been lately studied by Singh *et al.* [15], focusing in particular on high spin states and their interpretation in terms of single proton-neutron interaction and phonon excitations of the core. Therefore, the present lifetime analysis provides valuable information, which can be used for further, more stringent tests of theoretical models in this mass region, where several interesting phenomena, such as transition from oblate to prolate shape, octupole collectivity, γ instability, etc., take place.

IV. THEORETICAL INTERPRETATION

In this section we discuss the theoretical interpretation of the $9/2^+$ state, both in ^{65}Cu and ^{67}Cu, by means of the particle-vibration (weak) coupling model (PVC) of Bohr and Mottelson [5,16]. The model, recently applied in Refs. [7,8] in connection with experiments performed on ^{47,49}Ca, allows in principle to describe the states in odd nuclei arising by coupling a phonon excitation of the even-even core nucleus with an unpaired particle/hole of the final system.

First, the properties of the low-lying states, in particular the 3^- phonon of the ^{64,66}Ni cores, have been obtained with microscopic HF-BCS plus QRPA calculations (cf. Refs. [17,18] for details), employing two different Skyrme parameter sets

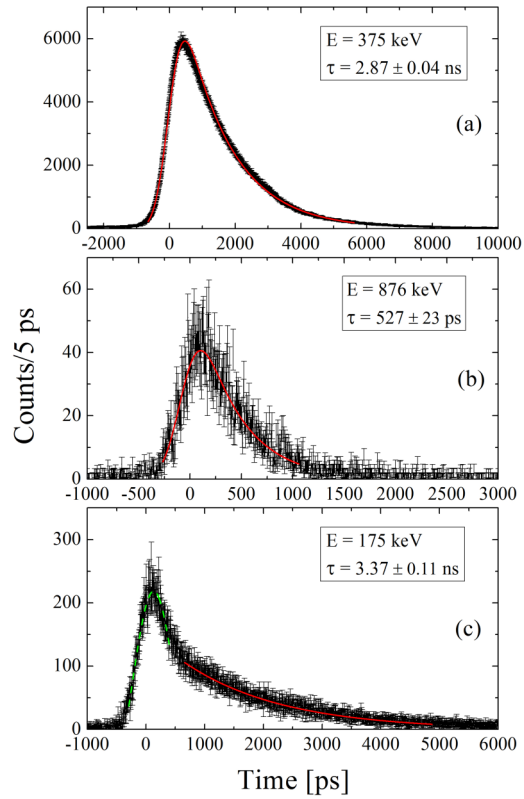

FIG. 7. (Color online) Example of time distribution spectra corresponding to three different lifetime values. (a)–(b): Time distribution of the 375 keV and 876 keV states of ^{68}Ga. The solid (red) line is the fit of the experimental data by the convolution function discussed in the text. (c) Time distribution of the 175 keV state of ^{68}Ga. The solid (red) line is the fit of the exponential component of experimental data while the dashed (green) line corresponds to the Gaussian component.

(SkX [19] and Sly5 [20]). For neutrons, the usual zero-range, density-dependent, pairing interaction

$$V_p(\vec{r}_1,\vec{r}_2) = V_0\left[1+\eta\left(\frac{\rho((\vec{r}_1+\vec{r}_2)/2)}{\rho_0}\right)^\gamma\right]\delta(\vec{r}_1-\vec{r}_2) \quad (1)$$

TABLE III. Energy and $B(E3)$ values of the 3^- phonon of ^{64}Ni (top), as calculated by the QRPA model with the SkX and Sly5 Skyrme forces, in comparison with the experimental values. Energy and $B(E3)$ values for the $9/2^+$ state of ^{65}Cu (bottom), as obtained either experimentally or by means of the PVC model (see text for details).

		E [MeV]	$B(E3)$ [W.u]
	^{64}Ni		
3^-	Expt.	3.560	10.83± 0.59
	Theory (SkX)	4.4	9.1
	Theory (Sly5)	5.2	9.8
	^{65}Cu		
$9/2^+$	Expt.	2.533	8.82 ± 1.65
	Theory (SkX)	3.1	6.2
	Theory (Sly5)	2.9	9.2

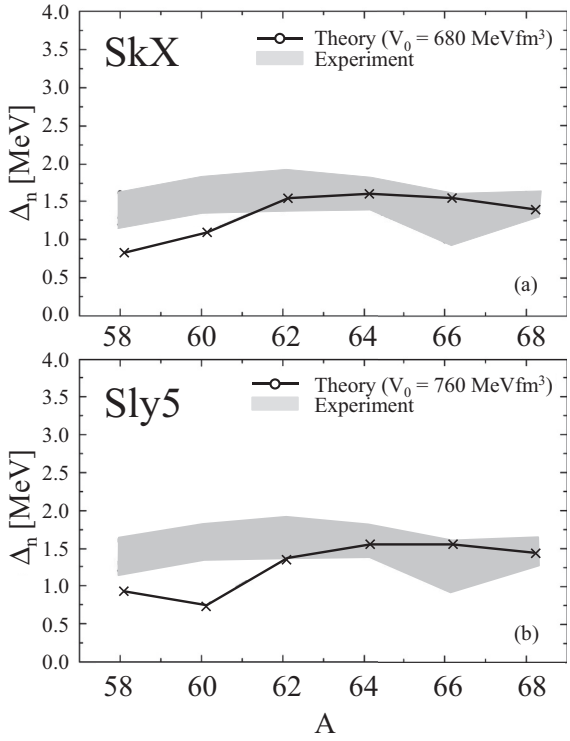

FIG. 8. Pairing gaps along the Ni isotopic chain. We compare empirical values (shaded areas), obtained by the three- and four-points formulas [5], and the theoretical HF-BCS calculations employing two different sets of Skyrme interactions SkX (a) and Sly5 (b).

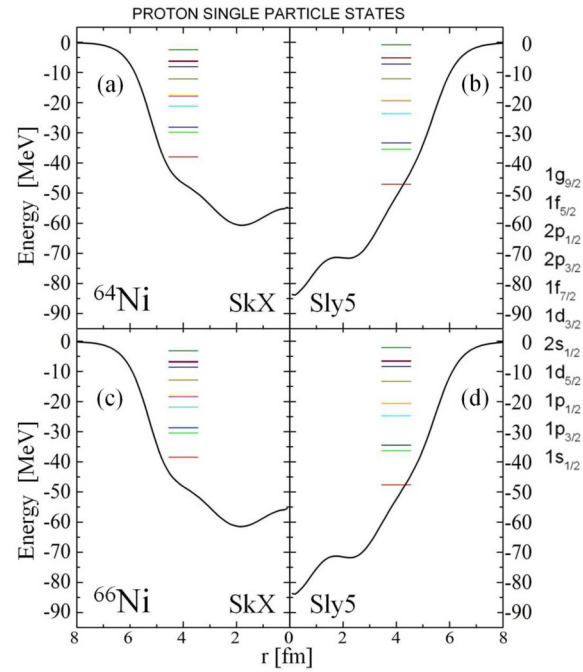

FIG. 9. (Color online) Proton single-particle states in ^{64}Ni (top), obtained by HF-BCS calculations performed with SkX (a) and Sly5 (b) Skyrme interactions, plotted together with the binding potential. Proton single-particle states in ^{66}Ni (bottom), obtained by HF-BCS calculations performed with SkX (c) and Sly5 (d) Skyrme interactions, plotted together with the binding potential. Labels for the corresponding proton single-particle states are given on the right of the figure.

is employed. $\vec{r}_1$,$\vec{r}_2$ are the spatial coordinates of the paired nucleons and ρ is the total density. ρ_0, γ and η (surface pairing), have been set 0.16 fm^{-3}, 1, and 1, for the sake of simplicity. The value of V_0 has been determined in order to reproduce reasonably the pairing gaps along the Ni isotopic chain, focusing in particular on the values obtained for ^{64,66}Ni. The results are shown in Fig. 8, where the shaded areas, corresponding to the empirical values obtained by the three- and four-points formulas [5], are plotted together with the theoretical calculations of this work. It was found that $V_0 = 680$ MeV and 760 MeV for the case of SkX and Sly5, respectively.

It is worth noting that the SkX interaction has been fitted on experimental single-particle states, in a similar mass region, using an effective mass close to the unity [19]. On the contrary, the Sly5 force is a typical interaction, which requires a smaller effective mass. With respect to this, it is shown in Fig. 9 a comparison between ^{64,66}Ni proton single-particle states, obtained by HF-BCS calculations employing both the sets of parameters.

Particle-vibration coupling calculations have then been performed for the $3^- \otimes \pi p3/2$ multiplet of ^{65}Cu, using the single-particle levels described in the previous paragraph. These calculations have been improved compared to the previous studies of ^{47,49}Ca, since, in addition to the lowest-order corrections to the energy of the states we now also include the lowest-order corrections to the $B(E3)$ (cf. the detailed formulas reported in Ref. [16]). These latter corrections tend to reduce the collectivity of the coupled states, as reported in Table III for the $9/2^+$ state of ^{65}Cu. A value of ≈8 W.u.

TABLE IV. Energy and $B(E3)$ values for the 3^- phonon of ^{66}Ni (top), as calculated by the QRPA model with the SkX and Sly5 Skyrme forces. The experimental value is available for the energy of the state only. Energy and $B(E3)$ values for the $9/2^+$ state of ^{67}Cu (bottom), as obtained either experimentally or by means of the PVC model (see text for details).

		E [MeV]	$B(E3)$ [W.u]
	^{66}Ni		
3^-	Expt.	3.371	– ⋆
	Theory (SkX)	4.1	7.9
	Theory (Sly5)	4.6	7.5
	^{67}Cu		
$9/2^+$	Expt.	2.503	16.8 ± 1.7
	Theory (SkX)	2.9	5.4
	Theory (Sly5)	2.9	5.2

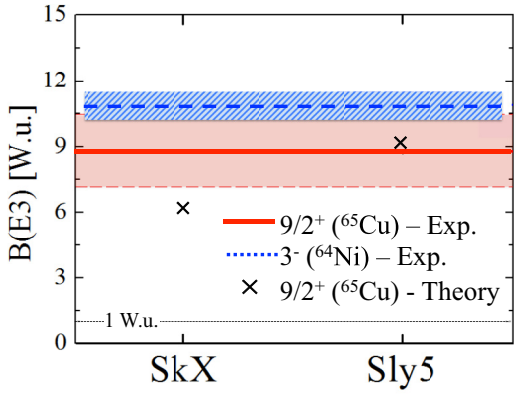

FIG. 10. (Color online) $B(E3)$ of the $9/2^+$ state of ^{65}Cu measured in the present work [solid (red) line] and the experimental error [shaded (red) area], compared with the theoretical calculations (cross symbols) performed with the SkX and SLy5 Skyrme interactions. As reference the dashed (blue) line and area represents the experimental adopted value and the error, respectively, of the 3^- phonon of ^{64}Ni core.

was obtained, which is in very good agreement with the experimental 8.8 ± 1.7 W.u., as shown in Fig. 10. Similar type of calculations have been performed for ^{67}Cu, recently measured at IFIN-HH by fast timing techniques [10]. In this case it is found that the calculated $B(E3)$ value is much smaller than the present experimental value, pointing to an anomalous behavior of the $9/2^+$ state in ^{67}Cu (Table IV), as compared, e.g., to lighter Cu isotopes.

V. CONCLUSION

In conclusion, this work shows the crucial role played by Cu isotopes to understand the interplay between single-particle degrees of freedom and collective vibrations [1] in terms, for example, of particle-vibration coupling. In particular, the discrepancy found between ^{65}Cu and ^{67}Cu offers a starting point for further theoretical investigations within the model, such as the inclusion of the coupling to more phonons and/or to paring vibrational modes.

ACKNOWLEDGMENTS

The work has been supported by Istituto Nazionale di Fisica Nucleare (INFN) and the Romanian UEFISCDI Contract No. PN-II-ID-PCE-2011-3-0367.

[1] I. Stefanescu, G. Georgiev, D. L. Balabanski, N. Blasi, A. Blazhev, N. Bree, J. Cederkall, T. E. Cocolios, T. Davinson, J. Diriken, J. Eberth, A. Ekstrom, D. Fedorov, V. N. Fedosseev, L. M. Fraile, S. Franchoo, K. Gladnishki, M. Huyse, O. Ivanov, V. Ivanov, J. Iwanicki, J. Jolie, T. Konstantinopoulos, T. Kroll, R. Krucken, U. Koster, A. Lagoyannis, G. LoBianco, P. Maierbeck, B. A. Marsh, P. Napiorkowski, N. Patronis, D. Pauwels, G. Rainovski, P. Reiter, K. Riisager, M. Seliverstov, G. Sletten, J. VandeWalle, P. VanDuppen, D. Voulot, N. Warr, F. Wenander, and K. Wrzosek, Phys. Rev. Lett. **100**, 112502 (2008).
[2] M. Asai, T. Ishii, A. Makishima, I. Hossain, M. Ogawa, and S. Ichikawa, Phys. Rev. C **62**, 054313 (2000).
[3] B. Zeidman and J. A. Nolen, Phys. Rev. C **18**, 2122 (1978).
[4] D. Bucurescu *et al.*, Nucl. Phys. A **189**, 577 (1972).
[5] A. Bohr, B. R. Mottelson, *Nuclear Structure*, Vols. I and II (W. A. Benjamin, San Francisco, 1975).
[6] P. F. Bortignon, A. Bracco, and R. A. Broglia, *Giant Resonances: Nuclear Structure at Finite Temperature* (Harwood Academic Publishers, New York, 1998).
[7] D. Montanari *et al.*, Phys. Lett. B **697**, 288 (2011).
[8] D. Montanari *et al.*, Phys. Rev. C **85**, 044301 (2012).
[9] N. Marginean *et al.*, Eur. Phys. J. A **46**, 329 (2010).
[10] C. R. Niţă *et al.*, Phys. Rev. C (to be published).
[11] C. J. Chiara *et al.*, Phys. Rev. C **85**, 024309 (2012).
[12] http://www.lnl.infn.it.
[13] T. Kibedi and R. H. Spear, At. Data Nucl. Data Tables **80**, 35 (2002).
[14] E. A. McCutchan, Nucl. Data Sheets **113**, 1735 (2012).
[15] A. K. Singh *et al.*, Eur. Phys. J. A **9**, 197 (2000).
[16] I. Hamamoto, Phy. Rep. **10**, 63 (1974).
[17] G. Colò *et al.*, Nucl. Phys. A **788**, 173c (2007).
[18] G. Colò *et al.*, Comput. Phys. Commun. **184**, 142 (2013).
[19] B. A. Brown, Phys. Rev. C **58**, 220 (1998).
[20] E. Chabanat, P. Bonche, P. Haensel, J. Meyer, and R. Schaeffer, Nucl. Phys. A **643**, 441 (1998).